Proceedings of the 6th International Conference on
Systems and Control, University of Batna 2, Batna,
Algeria, May 7-9, 2017

# Sliding mode control of reactive power for Three-Phase Grid-Connected Photovoltaic System.

Amal MARREKCHI, Soulaymen KAMMMOUN, Souhir SALLEM, MBA KAMMON

*Abstract*— **In Grid-Connected PV system should not be limited injecting the active power into the grid. However, it must be able to absorb or to generate sufficient reactive power for a certain amount of time according to the grid demand and maintain the grid voltage. This paper proposes sliding mode control that controls powers respectively the active and the reactive power for a Three-Phase Grid-Connected PV System. The sliding mode control based on dq transformation, after determining the desired voltage of the inverter $V_q$and $V_d$ in the rotating frame, which means a reactive power quantity that defines the angle phase between the grid current and voltage. This controller is simulated on a 10 MW PV generator system using Matlab/SIMULINK. According to the simulation results prove the efficiency and robustness of the sliding mode control to regulate the injected reactive power.**

***Keywords—Sliding mode control, Three phase grid, Photovoltaic System, power control***

## I. INTRODUCTION

Recently, many research trends in renewable energy management, modelling, energy conversion and power control analysis of distributed generation sources. The huge increase of grid connected PV generation systems may make some challenges to maintain stability of the grid, power quality and mismatch, power control and energy management... [1] and [2].

Several power control strategies for three-phase grid connected PV systems have been developed and handled in the literature [3], [4], [5], [6]and [7]. The purpose of these control strategies leads to regulate on the one hand the active power using the topology of maximum power point tracking (MPPT) and to maintain on the other hand a unit power factor.

This paper aims to control the DC/AC converter (inverter) in order to provide or to absorb reactive power from the grid and at the same time to improve its power quality. As a result, the AC modules with the reactive power management function is presented and developed on this paper. Among a variety kinds of control technologies, the present work proposes the sliding mode control to inject maximum power to the grid with providing or absorbing reactive power depending on the grid needs.

This paper is distributed as follows. The second section presents the proposed configuration and the modeling of the photovoltaic system connected to the grid. The proposed sliding mode control is developed and detailed in third section. In the fourth section, simulation results are shown and discussed. In the last section presents the conclusions.

## II. PV SYSTEM MODELING

The proposed configuration of three-phase grid connected photovoltaic system is presented in fig 1. It's composed of photovoltaic generator, two power-conditioning stages, LCL filter and three-phase grid. To match the required power, the solar modules are connected in a series and parallel configuration. A Boost chopper is employed to raise the DC voltage and extract the maximum of power from the GPV. The three-phase full-bridge inverter converts the continuous voltage into sinusoidal voltage and ensure that the current respect the needs of the grid.

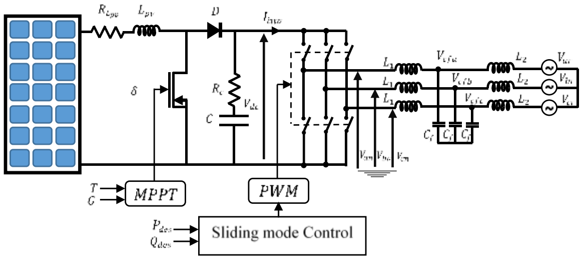

Fig. 1. Schema of proposed grid connected PV system.

### A. PVG modeling

The PVG consists of $N_s$ series module and $N_p$ parallels panels. Every module is constituted of $N_{sc}$ solar cell connected in series. The mathematical equation for the current of two-diode model is given as follows [8], [9], [10]and [11].

$$I_{PVG} = N_p I_{ph} - N_p I_o \left[ exp\left(\frac{V_{PVG}+\frac{N_s}{N_p}R_s I_{PVG}}{N_s N_{cs} a_1 V_T}\right) + exp\left(\frac{V_{PVG}+\frac{N_s}{N_p}R_s I_{PVG}}{N_s N_{cs} a_2 V_T}\right) - 2\right] - \frac{\left(V_{PVG}\frac{N_p}{N_s}+I_{PVG}R_s\right)}{R_p} \quad (1)$$

The reverse saturation current is given by the equation (2).

$$I_0 = \frac{I_{sc\_STC}+\alpha_{sc}\,\Delta T}{\exp\left[\frac{V_{oc\_STC}+\beta_{oc}\,\Delta T}{V_T}\right]-1} \quad (2)$$

Equation (3) describes the current generated by the incidence of light [12]:

$$I_{ph} = (I_{ph_{STC}} + \alpha_{sc}\Delta T)\frac{G}{G_{STC}} \quad (3)$$

---

* Research laboratory : Commande des Machines Electriques et Reseaux de puissance (CMERP)
National Engineering school of Sfax, ENIS, Sfax, Tunisia
e-mail: amal.marrekchi@gmail.com
e-mail :soulaymen.kammoun@gmail.com
e-mail :souhirsallem@gmail.com
e-mail :mbakammoun@gmail.com

Where $V_T = {}^{KT}\!/_{q}$, $\mathrm{I_{phSTC}}$ is the light generated current at STC (approximately $\mathrm{I_{phSTC}} = \mathrm{I_{scSTC}}$ [3]), $\Delta\mathrm{T} = \mathrm{T} - \mathrm{T_{STC}}$ ( $T_{STC} = 298K$), G present the solar irradiance, ($G_{STC} = 1000\ W/m^2$), a1 and a2 represent respectively the ideality factor of diode 1 and 2.

Figure 2 shows the equivalent circuit of two-diode model of solar cell [13].

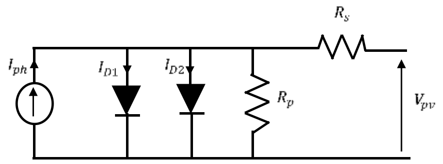

Fig. 2. Electrical schema of two diode model.

### B. Boost converter modeling

The DC/DC converter is presented by the following state space model Eq(4) [9].

$$\begin{cases} \frac{di_{Lpv}}{dt} = \frac{V_{pv}}{L_{pv}} - \left(\frac{R_{lpv}}{L_{pv}} i_{Lpv}\right) - (1-\delta)\left[\frac{R_c}{L_{pv}} i_{Lpv} - R_c I_{inv} + \frac{V_c}{L_{pv}}\right] \\ \frac{dV_c}{dt} = \frac{1}{C}(I_c - I_{inv}) \\ V_{dc} = I_c R_c + V_c \\ I_c = (1-\delta) i_{Lpv} \end{cases} \tag{4}$$

To extract the maximum of power from the PVG we propose a new algorithm is to find the MPPT based on the climatic parameters (irradiation and temperature). A current desired function is then generated and implanted in a micro controller in order to control the system to work in MPP for each couple ($G$, $T$) using a regulation loop on the current generated by the PV Array making this last generates the desired current [9].

### C. Three-phase inverter modeling

The model of three-phase inverter connected to the grid is given by the following equations [7].

$$\begin{bmatrix} V_{an} \\ V_{bn} \\ V_{cn} \end{bmatrix} = \frac{V_{dc}}{3} \begin{bmatrix} 2 & -1 & -1 \\ -1 & 2 & -1 \\ -1 & -1 & 2 \end{bmatrix} \begin{bmatrix} f_1 \\ f_2 \\ f_3 \end{bmatrix} \tag{5}$$

Where $f_1$, $f_2$ and $f_3$ are the PWM signals.

The modeling of the inverter coupled to the grid through an LCL filter is given by these equations. Equation (6) gives the three currents in the side of the inverter.

$$L_1 \frac{d}{dt} \begin{bmatrix} i_{L1a} \\ i_{L1b} \\ i_{L1c} \end{bmatrix} = \begin{bmatrix} V_{an} \\ V_{bn} \\ V_{cn} \end{bmatrix} - \begin{bmatrix} V_{cfa} \\ V_{cfb} \\ V_{cfc} \end{bmatrix} \tag{6}$$

The voltage of the filter capacitor is given by equation (7)

$$C_f \frac{d}{dt} \begin{bmatrix} V_{cfa} \\ V_{cfb} \\ V_{cfc} \end{bmatrix} = \begin{bmatrix} i_{L1a} \\ i_{L1b} \\ i_{L1c} \end{bmatrix} - \begin{bmatrix} i_{L2a} \\ i_{L2b} \\ i_{L2c} \end{bmatrix} \tag{7}$$

The injected current is described by the following equations.

$$L_2 \frac{d}{dt} \begin{bmatrix} i_{L2a} \\ i_{L2b} \\ i_{L2c} \end{bmatrix} = \begin{bmatrix} V_{cfa} \\ V_{cfb} \\ V_{cfc} \end{bmatrix} - \begin{bmatrix} V_{ar} \\ V_{br} \\ V_{cr} \end{bmatrix} \tag{8}$$

Applying transform Park, our system becomes as following (Eq (9), Eq (10), Eq (11)).

$$L_1 \frac{d}{dt} \begin{bmatrix} i_{L1d} \\ i_{L1q} \end{bmatrix} = \begin{bmatrix} V_d \\ V_q \end{bmatrix} - \begin{bmatrix} V_{cfd} \\ V_{cfq} \end{bmatrix} - \frac{3}{2} \omega\, L_1 \begin{bmatrix} -i_{L1q} \\ i_{L1d} \end{bmatrix} \tag{9}$$

$$C_f \frac{d}{dt} \begin{bmatrix} V_{cfd} \\ V_{cfq} \end{bmatrix} = \begin{bmatrix} i_{L1d} \\ i_{L1q} \end{bmatrix} - \begin{bmatrix} i_{L2d} \\ i_{L2q} \end{bmatrix} - \frac{3}{2} \omega\, C_f \begin{bmatrix} -V_{cfq} \\ V_{cfd} \end{bmatrix} \tag{10}$$

$$L_2 \frac{d}{dt} \begin{bmatrix} i_{L2d} \\ i_{L2q} \end{bmatrix} = \begin{bmatrix} V_{cfd} \\ V_{cfq} \end{bmatrix} - \begin{bmatrix} V_{dr} \\ V_{qr} \end{bmatrix} - \frac{3}{2} \omega\, L_2 \begin{bmatrix} -i_{L2q} \\ i_{L2d} \end{bmatrix} \tag{11}$$

The instantaneous powers which are delivered to the grid are given by equations 12.

$$\begin{cases} P = \frac{2}{3} V_{qr} i_{L2q} \\ Q = \frac{2}{3} V_{qr} i_{L2d} \end{cases} \tag{12}$$

## III. PROPOSED CONTROL

For the proposed three phase grid connected to PV generator, our purpose is to obtain the maximum of power extracted from the PVG and the reactive power at its reference value. Our objective is to have fast dynamics to follow as quickly as possible the reference power with high disturbance rejection. Therefore, the use of sliding mode control seems to be suitable since the studied system is strongly nonlinear. In fact, the sliding surface is composed by the linear combination of state variable errors that are defined as the differences between the state variables and their references. The synthesis of a command by sliding mode is realized in three steps [14]:

- The choice of suitable sliding surface,
- Development of convergence conditions,
- Determination of the control law

In our case, the sliding surface must be designed to control the currents injected into the grid $i_{L2d}$ and $i_{L2q}$. The convergence conditions can be obtained by selecting a sliding surface using only the errors of the injected currents. The reference injected currents can be expressed by a function proportional to the active and reactive power (13).

$$\left\{ i^*_{L2q} = \frac{2}{3V_{rq}} P^* \middle| i^*_{L2d} = \frac{2}{3V_{rq}} Q^* \right\} \tag{13}$$

The proposed errors are given by (14)

$$\left\{ e_1 = i_{L2d} - i^*_{L2d} \middle| e_2 = i_{L2q} - i^*_{L2q} \right\} \tag{14}$$

Where $C_1$ and $C_2$ are positive constants. The sliding mode dynamics must be verified this equality $C_1 e_1 + C_2 \dot{e_1} + \ddot{e_1} = 0$ to be stable globally.

The derivates of the first error $e_1$ are given as follows:

$$\dot{e_1} = -\dot{\iota_{L2d}} = -\left[\frac{V_{cfd}}{L_2} + \frac{3}{2} \omega i_{L2q}\right] \tag{15}$$

$$\ddot{e_1} = -\left[\frac{\dot{V_{cfd}}}{L_2} + \frac{3}{2}\omega \dot{\iota_{L2q}}\right] = i_{L2d}\left[\frac{1}{C_f L_2} + \frac{9}{4}\omega^2\right] - \frac{3\omega}{L_2}V_{cfq} + \frac{3\omega}{2L_2}V_{qr} - \frac{i_{L1d}}{C_f L_2} \quad (16)$$

$$\begin{cases} e_1^{(3)} = \dot{\iota_{L2d}}\left[\frac{1}{C_f L_2} + \frac{9}{4}\omega^2\right] - \frac{3\omega}{L_2}\dot{V_{cfq}} - \frac{\dot{\iota_{L1d}}}{C_f L_2} \\ e_1^{(3)} = \dot{\iota_{L2d}}\left[\frac{1}{C_f L_2} + \frac{9}{4}\omega^2\right] - \frac{3\omega}{L_2}\dot{V_{cfq}} - \frac{1}{C_f L_2 L_1}V_d + \frac{1}{C_f L_2 L_1}V_{cfd} - \frac{3\omega}{2C_f L_2}i_{L1q} \end{cases} \quad (17)$$

The derivates of the second error $e_2$ are given as follows:

$$\dot{e_2} = -\dot{\iota_{L2q}} = -\left[\frac{V_{cfq}}{L_2} - \frac{3}{2}\omega i_{L2d} - \frac{V_{rq}}{L_2}\right] \quad (18)$$

$$\ddot{e_2} = -\left[\frac{\dot{V_{cfq}}}{L_2} - \frac{3}{2}\omega \dot{\iota_{L2d}}\right] = i_{L2q}\left[\frac{1}{C_f L_2} + \frac{9}{4}\omega^2\right] + \frac{3\omega}{L_2}V_{cfd} - \frac{i_{L1q}}{C_f L_2} \quad (19)$$

$$e_2^{(3)} = \dot{\iota_{L2q}}\left[\frac{1}{C_f L_2} + \frac{9}{4}\omega^2\right] + \frac{3\omega}{L_2}\dot{V_{cfd}} - \frac{V_q}{C_f L_2 L_1} + \frac{V_{cfq}}{C_f L_2 L_1} + \frac{3\omega}{2\,C_f L_2}i_{L1d} \quad (20)$$

The vectors control $V_d$ and $V_q$ appear in the third derivative. The sliding surface must be globally stable, which implies $S1 = 0$ and $S2 = 0$. The derivatives of the two sliding surfaces must also be equals to zero and $V_d^N = 0$ and $V_q^N = 0$. During the convergence mode, we must verify the condition $S\dot{S} < 0$, we choose the derivate of surface equal to equation (21).

$$\{\dot{S}1 = -M\,S1 - Nsign(S1) | \dot{S}2 = -M\,S2 - Nsign(S2)\} \quad (21)$$

Then we can obtain the two control lows as follows:

$$\begin{cases} V_d = C_f L_2 L_1 \left[ \begin{matrix} M\,S1 + Nsign(S1) + \dot{\iota_{L2d}}\left[\frac{1}{C_f L_2} + \frac{9}{4}\omega^2\right] \\ -\frac{3\omega}{L_2}\dot{V_{cfq}} + \frac{V_{cfd}}{C_f L_2 L_1} - \frac{3\omega}{2C_f L_2}i_{L1q} \end{matrix} \right] \\ V_q = C_f L_2 L_1 \left[ \begin{matrix} M\,S + Nsign(S2) + \dot{\iota_{L2q}}\left[\frac{1}{C_f L_2} + \frac{9}{4}\omega^2\right] \\ +\frac{3\omega}{L_2}\dot{V_{cfd}} + \frac{V_{cfq}}{C_f L_2 L_1} + \frac{3\omega}{2\,C_f L_2}i_{L1d} \end{matrix} \right] \end{cases} \quad (22)$$

Figure 3 presents the adopted sliding mode control for three phase grid connected PVG.

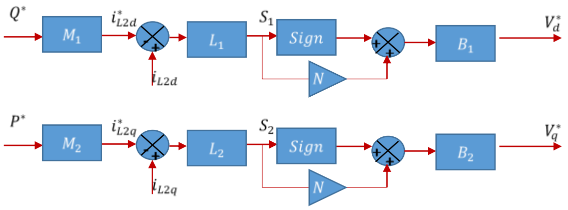

Fig. 3. Block diagram of the Sliding mode control.

Where $M$ and $N$ are two positive constants.

$$M_1 = M_2 = \frac{2}{3V_{rq}};\ B_1 = B_2 = C_f L_1 L_2;$$

$$L_1 = \dot{\iota_{L2d}}\left[\frac{1}{C_f L_2} + \frac{9}{4}\omega^2\right] - \frac{3\omega}{L_2}\dot{V_{cfq}} + \frac{V_{cfd}}{C_f L_2 L_1} - \frac{3\omega}{2C_f L_2}i_{L1q}$$

and

$$L_2 = \dot{\iota_{L2q}}\left[\frac{1}{C_f L_2} + \frac{9}{4}\omega^2\right] + \frac{3\omega}{L_2}\dot{V_{cfd}} + \frac{V_{cfq}}{C_f L_2 L_1} + \frac{3\omega}{2\,C_f L_2}i_{L1d}$$

The inverter input must be maintained constant DC voltage. In fact, we propose to add a proportional integral corrector. It is parameterized as a function of the value of the capacitor and the dynamics of the control loop. Figure 4 shows the control loop of DC link.

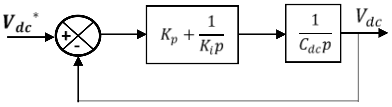

Fig. 4. DC link voltage regulator.

## IV. RESULTS AND DISCUSSION

To prove more the performance and the efficiency of the proposed control, we simulate the model of three-phase grid-connected to a PVG equal to 10MW ( $N_s = 334$ $and$ $N_p = 500$) in MATLAB/Simulink. We consider that the PVG is connected to the grid and all conditions before coupling are verified [9]. The model parameters are defined and presented in table1. Simulation results are given for various (G,T) couples presented in Fig 5.

Table 1: Characteristics of the BP MSX60 in standard conditions ($G = 1000\ W/m^2$ $and$ $T = 25°C$).

| | |
|---|---|
| $V_{oc}$ in V | 21 |
| $I_{sc}$ in A | 3,74 |
| $V_{mp}$ in V | 17,1 |
| $I_{mp}$ in A | 3,5 |
| $P_{mp}$ in W | 60 |
| $\beta_{oc}$ in mV/°C | - 80 |
| $\alpha_{sc}$ in mA/°C | 2,47 |

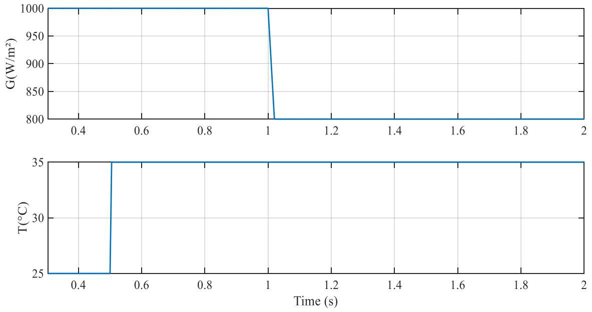

Fig. 5. Climatic conditions profiles.

Figure 6 illustrates desired and measured output current of the PVG. We can clearly see that the output current of the PVG follows the desired one which is maintained to MPPT current.

Following to fig. 6, this current is sensitive to irradiation perturbation. In fact, at $t = 1s$ , the irradiance decreases from $1000W/m^2$ $until$ $800W/m^2$, the output GPV MPPT current then decreases in the same way.

Figure 7 shows the response of output voltage of the PVG. It is obvious that the PVG voltage is sensitive to the temperature variation. We can note that the proposed MPPT control yields to accurate values of current and voltage and adapts the new value of current and voltage refer to maximum power point when the climatic conditions changes. Figure 8 shows the evolution of the voltage of the DC bus. We can see that the DC bus is stable even when the climatic condition changes. This is due to the DC bus regulator which adapts always the same value of the DC bus voltage.

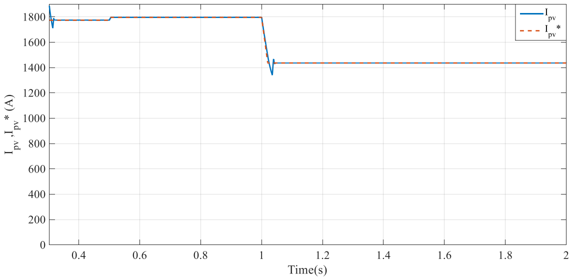

Fig. 6. Evolution of the output current of the PV generator for given G and T.

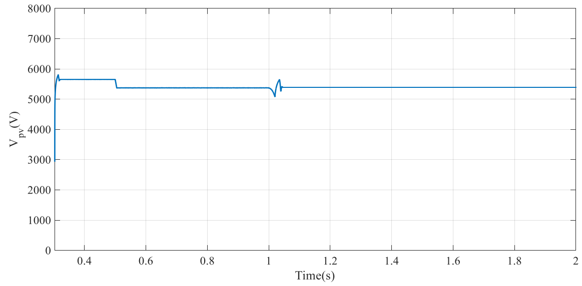

Fig. 7. Evolution of the output voltage of the PV generator for given G and T.

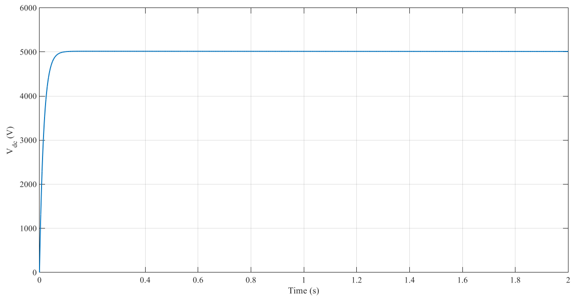

Fig. 8. Evolution of the DC bus voltage.

Figure 9 and figure 10 illustrate respectively the active and reactive power compared to the desired ones. In our application, the desired active power is the maximum power extracted from the PVG. It is obvious from figure 9 that the injected active power follows the desired power under various climatic conditions. As showing in figure 10, we can inject or absorb the reactive power which does not exceed 30% of the active power. The two figures are showing the excellent tracking of the reference. We can from these figures that the sliding mode control is robust and efficient for this application.

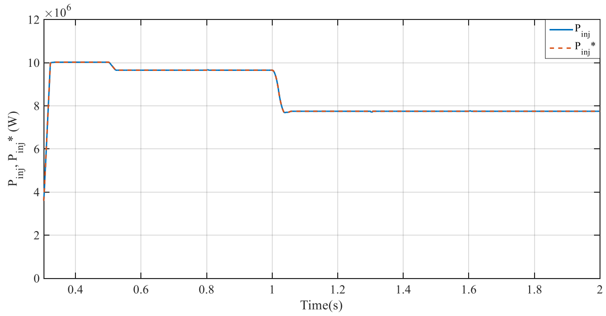

Fig. 9. Evolution of the active power injected to the grid.

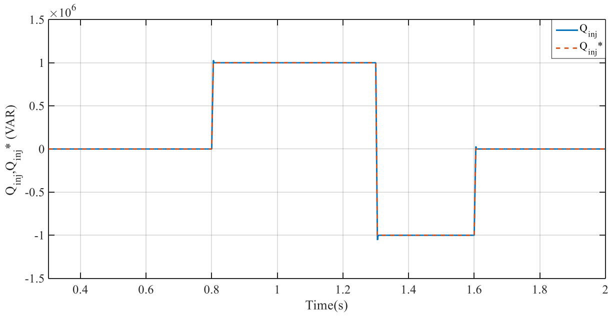

Fig. 10. Evolution of reactive power injected to the grid.

Figure 11 shows the output three-phase voltage and the injected current into the grid. As can be seen in the zoom of figure 11 (a), the use of LCL filter offers a high quality of injected current.

Figure 12 illustrates the output voltage and the injected current of the first phase of the grid. Figure 12 explains the reactive power flux for three modes: the reactive power absorption (Q>0), reactive power zero and reactive power injection (Q<0). In fact, figure 12 (a) illustrates the output voltage and injected current in the first phase of the grid. Figure 12 (b), 12(c) and 12(d) show a zoom of the figures 12(a) and Figure 12 (e) plot the evolution of the phase delay, as a consequence of the three-operating mod as follows:

- For $0 < t < 0.8\ s$ , no reactive power is injected to the grid ($Q = 0$). In this case, the voltage and the current outputs are in phase (Fig.12 b).
- For $0.8 < t < 1.3\ s$ , the reactive power is absorbed from the grid ($Q < 0$). In this case, the voltage is in advance with respect to the current (Fig.12 c).
- For $1.3 < t < 1.6\ s$ , the reactive power is injected to the grid ($Q > 0$). In this case, the current is in advance with respect to the voltage (Fig.12 d).

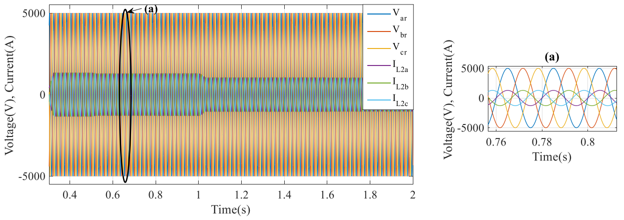

Fig. 11 Three-phase voltage and the current injected of grid side.

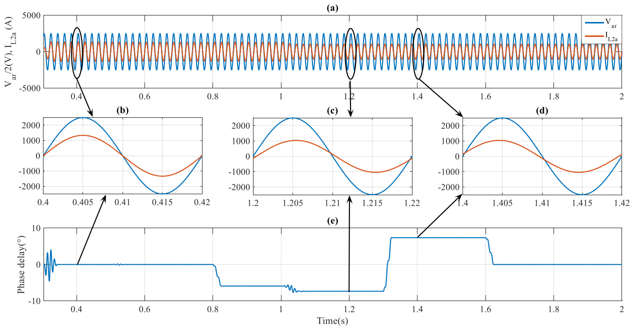

Fig. 12 (a)First phase voltage of the grid and the injected current
(b) Voltage and current in the first phase when (Q=0)
(c) Voltage and current in the first phase when (Q<0)
(d) Voltage and current in the first phase when (Q>0)
(e) Evolution of the phase delay of the first phase.

As it is seen, different results demonstrate the effectiveness of the integrated control strategy in terms of precision , rapidity and stability.

## V. CONCLUSION

In this paper, a three-phase grid connected to photovoltaic generator is modeled and simulated by MATLAB. All the elements of the proposed system were clearly described and modelled in order to obtain satisfactory results. The boost converter has the roll of extraction the maximum of the PVG power. A sliding mode control was proposed to regulate the injected active and reactive power. The purpose of the sliding mode is to inject the maximum of active power produced from the PVG in one hand and to inject or absorb the reactive power according to the needs of the grid. On another hand the simulation results illustrate that sliding mode control offers an excellent response during the climatic condition changes. The reactive power changes according to the needs of the grid which can inject, absorb or have the unit power factor.

## NOMENCLATURE

| | | |
|---|---|---|
| PV | : | Photovoltaic |
| PVG | : | Photovoltaic generator |
| MPPT | : | Maximum Power Point Tracking |
| MPP | : | Maximum Power Point |
| DC | : | Direct Current |
| $I_{pv}$ | : | PV cell current |
| $I_{ph}$ | : | Current generated by the incidence of light |
| $I_{D1}$ | : | Diode 1 current |
| $I_{D2}$ | : | Diode 2 current |
| $R_s$ | : | Series resistance of the PV cell equivalent circuit |
| $R_p$ | : | Shunt resistance of the PV cell equivalent circuit |
| $V_{pv}$ | : | PV cell voltage |
| $\alpha_{sc}$ | : | Short-circuit current coefficient |
| $\beta_{oc}$ | : | Open-circuit voltage coefficient |
| STC | : | Standard Test Conditions |
| $V_T$ | : | Thermal voltage |
| $I_{01}$ | : | Diode 1 reverse saturation current |
| $I_{02}$ | : | Diode 2 reverse saturation current |
| $a_1$ | : | Diode 1 ideality constant |
| $a_2$ | : | Diode 2 ideality constant |
| q | : | The electron charge |
| k | : | Boltzmann constant |
| $N_{sc}$ | : | Number of cells connected in series |
| $N_s$ | : | Number of modules connected in series in each branch |
| $N_p$ | : | Number of parallel branches in the PVG |
| $I_{pvg}$ | : | PVG current |
| $V_{pvg}$ | : | PVG voltage |
| $L_1$ | : | Filter inductance in the side of the inverter |
| $L_2$ | : | Filter inductance in the side of the grid |
| $C_f$ | : | Filter capacitor |
| $V_{ar}, V_{br} and\ V_{cr}$ | : | Voltage of the grid |
| $V_{an}, V_{bn} and\ V_{cn}$ | : | Output voltage of the inverter |
| $V_{cfa}, V_{cfb} and\ V_{cfc}$ | : | Voltage of the filter capacitor |
| $I_{L1a}, I_{L1b} and\ I_{L1c}$ | : | Output current of the inverter |
| $I_{L2a}, I_{L2b} and\ I_{L2c}$ | : | Injected current in the grid |
| δ | : | Duty cycle |

## REFERENCES

[1] S.DHAR, P.K. DASH, “A NEW BACKSTEPPING FINITE TIME SLIDING MODE CONTROL OF GRID CONNECTED PV SYSTEM USING MULTIVARIABLE DYNAMIC VSC MODEL”, INTERNATIONAL JOURNAL OF ELECTRICAL POWER & ENERGY SYSTEMS,VOL 82, NOVEMBER 2016, PAGES 314–330

[2] IF. BLAABJERG, R. TEODORESCU, M. LISERRE, A.V. TIMBUS, “OVERVIEW OF CONTROL AND GRID SYNCHRONIZATION FOR DISTRIBUTED POWER GENBERATION SYSTEM”,IEEE TRANS INDUST ELECTRON,VOL 53, 2006, PP. 1398–1409.

[3] FADIL, H.E., GIRI, F., GUERRERO, J.M., “GRID-CONNECTED OF PHOTOVOLTAIC MODULE USING NONLINEAR CONTROL”, 3RD IEEE INTERNATIONAL SYMPOSIUM ON POWER ELECTRONICS FOR DISTRIBUTED GENERATION SYSTEMS (PEDG), JUNE 2012, PP.119-124, 25-28

[4] IL-SONG KIM, “SLIDING MODE CONTROLLER FOR THE SINGLE-PHASE GRID-CONNECTED PHOTOVOLTAIC SYSTEM,” APPLIED ENERGY , VOL83, 2006, PP 1101–1115.

[5] RENUKADEVI V, B. JAYANAND, “HARMONIC AND REACTIVE POWER COMPENSATION OF GRID CONNECTED PHOTOVOLTAIC SYSTEM”, PROCEDIA TECHNOLOGY, VOLUME 21, 2015, PP 438–442.

[6] HUAJUN YU, JUNMIN PAN, AN XIANG, “A MULTI-FUNCTION GRID-CONNECTED PV SYSTEM WITH REACTIVE POWER COMPENSATION FOR THE GRID”, SOLAR ENERGY, VOL 79, JULY 2005, PP 101–106

[7] LEONARDO P. SAMPAIO, MOACYR A.G. DE BRITO , GUILHERME DE A. E MELO , CARLOS A. CANESIN, “GRID-TIE THREE-PHASE INVERTER WITH ACTIVE POWER INJECTION AND REACTIVE POWER COMPENSATION”, RENEWABLE ENERGY, VOL85 ,2016, PP 854-864.

[8] C. AOUADI, A. ABOULOIFA, A. HAMDOUN, Y. BOUSSAIRI “BACKSTEPPING BASED CONTROL OF PV SYSTEM CONNECTED TO THE GRID”, INTERNATIONAL JOURNAL OF COMPUTER AND INFORMATION TECHNOLOGY, VOL 03 , SEPTEMBER 2014, PP 1021-1026.

[9] AMAL MARREKCHI, SOULAYMEN KAMMOUN, SOUHIR SALLEM, MOHAMED BEN ALI KAMMOUN, “A PRACTICAL TECHNIQUE FOR CONNECTING PV GENERATOR TO SINGLE-PHASE GRID”, SOLAR ENERGY, VOL 118, AUGUST 2015, PP 145–154.

[10] SOUHIR SALLEM, AMAL MARREKCHI, SOULAYMEN KAMMOUN, AND MOHAMED BEN ALI KAMMOUN, “MULTI-PV TECHNOLOGIES METHOD FOR PARAMETERS ESTIMATION OF TWO-DIODE MODEL”, THE EUROPEAN PHYSICAL JOURNAL PLUS, DECEMBER 2016.

[11] KASHIF ISHAQUE, ZAINAL SALAM, HAMED TAHERI, SYAFARUDDIN, “MODELING AND SIMULATION OF PHOTOVOLTAIC (PV) SYSTEM DURING PARTIAL SHADING BASED ON A TWO-DIODE MODEL”, SIMULATION MODELLING PRACTICE AND THEORY, VOL 19 , 2011, PP 1613–1626.

[12] KASHIF ISHAQUE, ZAINAL SALAM, AMIR SHAMSUDIN, MUHAMMAD AMJAD, “A DIRECT CONTROL BASED MAXIMUM POWER POINT TRACKING METHOD FOR PHOTOVOLTAIC SYSTEM UNDER PARTIAL SHADING CONDITIONS USING PARTICLE SWARM OPTIMIZATION ALGORITHM”, APPLIED ENERGY, VOL 99 , 2012,PP 414–422.

[13] LOTFI KHEMISSI, BRAHIM KHIARI, RIDHA ANDOULSI, ADNANE CHERIF, “ LOW COST AND HIGH EFFICIENCY OF SINGLE PHASE PHOTOVOLTAIC SYSTEM BASED ON MICROCONTROLLER”, SOLAR ENERGY, VOL 86, 2012, PP 1129–1141.

[14] IL-SONG KIM, “SLIDING MODE CONTROLLER FOR THE SINGLE-PHASE GRID-CONNECTED PHOTOVOLTAIC SYSTEM”, APPLIED ENERGY, VOL 83, OCTOBER 2006, PP 1101–1115.